Monthly Notices
of the
ROYAL ASTRONOMICAL SOCIETY

Mon. Not. R. Astron. Soc. **424,** 1807–1816 (2012) doi:10.1111/j.1365-2966.2012.21274.x

The VMC survey – V. First results for classical Cepheids⋆

V. Ripepi,[1]† M. I. Moretti,[2,3] M. Marconi,[1] G. Clementini,[2] M.-R. L. Cioni,[4,5]‡ J. B. Marquette,[6] L. Girardi,[7] S. Rubele,[7] M. A. T. Groenewegen,[8] R. de Grijs,[9,10] B. K. Gibson,[11,12,13] J. M. Oliveira,[14] J. Th. van Loon[14] and J. P. Emerson[15]

[1]*INAF–Osservatorio Astronomico di Capodimonte, Via Moiariello 16, 80131, Naples, Italy*
[2]*INAF–Osservatorio Astronomico di Bologna, via Ranzani 1, Bologna, Italy*
[3]*Department of Astronomy, University of Bologna, via Ranzani 1, 40127, Bologna, Italy*
[4]*School of Physics Astronomy and Mathematics, University of Hertfordshire, Hatfield AL10 9AB*
[5]*University Observatory Munich, Scheinerstrasse 1, 81679 Munich, Germany*
[6]*UPMC–CNRS, UMR7095, Institut d'Astrophysique de Paris, F-75014, Paris, France*
[7]*INAF–Osservatorio Astronomico di Padova, Vicolo dell'Osservatorio 5, 35122 Padova, Italy*
[8]*Koninklijke Sterrenwacht van België, Ringlaan 3, 1180, Brussel, Belgium*
[9]*Kavli Institute for Astronomy and Astrophysics, Peking University, Yi He Yuan Lu 5, Hai Dian District, Beijing 100871, China*
[10]*Department of Astronomy and Space Science, Kyung Hee University, Yongin-shi, 449-701, Kyungki-do, Republic of Korea*
[11]*Jeremiah Horrocks Institute, University of Central Lancashire, Preston PR1 2HE*
[12]*Department of Astronomy and Physics, Saint Mary's University, Halifax, Nova Scotia, B3H 3C3, Canada*
[13]*Monash Centre for Astrophysics, School of Mathematical Sciences, Monash University, Clayton, VIC 3800, Australia*
[14]*Astrophysics Group, Lennard-Jones Laboratories, Keele University, Staffordshire ST5 5BG*
[15]*Astronomy Unit, School of Physics and Astronomy, Queen Mary University of London, Mile End Road, London E1 4NS*

Accepted 2012 May 9. Received 2012 May 5; in original form 2012 April 8

ABSTRACT

The VISTA Magellanic Cloud (VMC; PI: M.-R. L. Cioni) survey is collecting deep K_s-band time series photometry of the pulsating variable stars hosted by the system formed by the two Magellanic Clouds (MCs) and the bridge connecting them. In this paper, we present the first results for classical Cepheids, from the VMC observations of two fields in the Large Magellanic Cloud (LMC), centred on the South Ecliptic Pole and the 30 Doradus star-forming regions, respectively. The VMC K_s-band light curves of the Cepheids are well sampled (12 epochs) and of excellent precision (typical errors of ∼0.01 mag). We were able to measure for the first time the K_s magnitude of the faintest classical Cepheids in the LMC ($K_s \sim 17.5$ mag), which are mostly pulsating in the first overtone (FO) mode, and to obtain FO period–luminosity (*PL*), period–Wesenheit (*PW*) and period–luminosity–colour (*PLC*) relations, spanning the full period range from 0.25 to 6 d. Since the longest period Cepheid in our data set has a variability period of 23 d, we have complemented our sample with literature data for brighter F Cepheids. On this basis, we have built a *PL* relation in the K_s band that, for the first time, includes short-period – hence low-luminosity – pulsators, and spans the full range from 1.6 to 100 d in period.We also provide the first ever empirical *PW* and *PLC* relations using the $(V - K_s)$ colour and time series K_s photometry. The very small dispersion (∼0.07 mag) of these relations makes them very well suited to study the three-dimensional geometry of the Magellanic system. The use of 'direct' (parallax- and Baade–Wesselink-based) distance measurements to both Galactic and LMC Cepheids allowed us to calibrate the zero-points of the *PL*, *PW* and *PLC* relations obtained in this paper, and in turn to estimate an absolute distance modulus of $(m - M)_0 = 18.46 \pm 0.03$ mag for the LMC. This result is in agreement with most of the latest literature determinations based on classical Cepheids.

Key words: surveys – stars: variables: Cepheids – galaxies: distances and redshifts – Magellanic Clouds.

⋆Based on observations made with VISTA at ESO under programme ID 179.B-2003.

†E-mail: ripepi@oacn.inaf.it
‡Research fellow at the Alexander von Humboldt Foundation.

© 2012 The Authors
Monthly Notices of the Royal Astronomical Society © 2012 RAS

1 INTRODUCTION

The Magellanic Clouds (MCs) represent a benchmark for studies of stellar populations and galactic evolution (see e.g. Harris & Zaritsky 2004, 2009). The Milky Way–Magellanic Cloud system is the closest example of a complex ongoing galaxy interaction (see e.g. Putman et al. 1998; Muller et al. 2004; Stanimirović, Staveley-Smith & Jones 2004; Bekki & Chiba 2007). Having a metallicity lower than the Galaxy and hosting significantly younger populous clusters, the MCs are also an important laboratory for testing the theory of stellar evolution (see e.g. Brocato et al. 2004; Neilson & Langer 2012).

Amongst extragalactic systems, the LMC represents the 'first step' of the extragalactic distance scale, thus holding a key role for the definition of the entire cosmic distance ladder (see e.g. Walker 2012 and references therein). Indeed, the absolute calibration of extragalactic distances obtained by the *Hubble Space Telescope* (*HST*) Key Project (Freedman et al. 2001) and the Supernovae Ia (SNIa) calibration team (see e.g. Saha et al. 2001) both rest upon an assumption of the distance to the LMC, and on the adoption of the *V*- and *I*-band period–luminosity (*PL*) relations of classical Cepheids in this galaxy. Any systematic effects in the distance to the LMC and/or in the slope of the Cepheid *PL* relations are expected to affect the final calibration of the cosmic distance scale and, in turn, the resulting estimate of the Hubble constant (see Marconi 2009; Bono et al. 2010; Walker 2012, and references therein).

The classical Cepheid *PL* relations have been demonstrated by several authors to show a non-negligible dependence on chemical composition (see e.g. Caputo, Marconi & Musella 2000; Romaniello et al. 2005, 2008; Marconi 2009; Bono et al. 2010; Freedman & Madore 2011) with the effect being significantly reduced at near-infrared (NIR) wavelengths (Bono et al. 1999; Caputo, Marconi & Musella 2000; Marconi, Musella & Fiorentino 2005; Marconi et al. 2010). The NIR bands are also less affected by reddening and, in these filters, the *PL* relations show a smaller intrinsic dispersion (see e.g. Madore & Freedman 1991; Caputo et al. 2000) and a much reduced non-linearity (Bono et al. 1999; Caputo et al. 2000; Marconi 2009) than in the optical range. Furthermore, pulsation amplitudes are much smaller in the NIR than in the optical bands, thus accurate mean magnitudes can be derived from a small number of phase points along the pulsation cycle. NIR observations of classical Cepheids, as well as of other pulsating stars (see e.g. Moretti et al. 2012, hereinafter M12), over the whole Magellanic system, including the bridge connecting the two clouds, are one of the key objectives of the VISTA near-infrared YJK_s survey of the Magellanic system (VMC; Cioni et al. 2011, hereinafter Paper I). This European Southern Observatory (ESO) public survey is obtaining deep NIR imaging in the *Y*, *J* and K_s filters of a wide area across the Magellanic system, using the VIRCAM (VIST IR camera; Dalton et al. 2006) of the ESO Visible and Infrared Survey Telescope for Astronomy (VISTA; Emerson, McPherson & Sutherland 2006). The main science goals of VMC are the determination of the spatially resolved star-formation history (SFH) and the definition of the three-dimensional (3D) structure of the whole Magellanic system. The observations are designed to reach $K_s \sim 20.3$ mag at a signal-to-noise ratio (S/N) of 10, in order to detect sources encompassing most phases of stellar evolution: from the main-sequence, to subgiants, upper and lower red giant branch (RGB) stars, red clump stars, RR Lyrae and Cepheid variables, asymptotic giant branch (AGB) stars, post-AGB stars, planetary nebulae (PNe), supernova remnants (SNRs), etc. These different stellar populations will enable the study of age and metallicity evolution within the whole MC system.

In this paper we present results for the classical Cepheids contained in the first two 'tiles' completely observed (the whole 12-epoch time series) by the VMC survey, namely tiles 8_8 and 6_6. Some preliminary results from the analysis of the classical Cepheids in these two tiles were published in Ripepi et al. (2012). Tile 8_8 is of particular interest, as it covers the South Ecliptic Pole (hereinafter SEP) region that the *Gaia* astrometric satellite (Lindegren & Perryman 1996; Lindegren 2010) will repeatedly observe for calibration purposes at the start of the mission, just after launch in Spring 2013. It is a tile that lies in an uncrowded, peripheral area of the LMC. Tile 6_6 is centred instead on the well-known 30 Doradus (hereinafter 30 Dor) star-forming region. It lies in the central part of the LMC and is a very crowded area.

The VMC data for the SEP and 30 Dor classical Cepheids are presented in Section 2. The K_s *PL*, *PW* and *PLC* relations derived from fundamental (F) and first-overtone (FO) classical Cepheids in these two LMC regions are discussed in Sections 3 and 4. The zero-point calibrations of the *PL*, *PW* and *PLC* relations based on a number of different methods are presented in Section 5. Our final estimate of the distance to the LMC based on the 30 Dor and SEP classical Cepheids is discussed in Section 6. Finally, a summary of the main results is presented in Section 7.

2 THE VMC DATA FOR THE VARIABLE STARS

The VMC observing strategy is described in detail in Paper I. The data acquisition procedures specifically applied to the variable stars, the cross-matching between the VMC and existing optical catalogues for the variable stars and the derivation of the information needed for their analysis are extensively discussed in M12. The interested reader is referred to these two papers for more details. Here, we briefly recall the main steps of the procedures applied to obtain the K_s light curves and $\langle K_s \rangle$ average magnitudes for the classical Cepheids in the 30 Dor and SEP fields.

In order to obtain well-sampled light curves, the VMC K_s-band time series observations were scheduled into 12 separate epochs distributed over ideally several consecutive months. The VMC data, processed through the pipeline (Irwin et al. 2004) of the VISTA Data Flow System (VDFS; Emerson et al. 2004), were retrieved from the VISTA Science Archive (VSA; Cross et al. 2012).[1] For our analysis we used the v20110909 VMC release 'pawprints' (six 'pawprints' form a 'tile'; see Paper I and M12). Since usually a variable star is observed in two or three not necessarily consecutive pawprints, we first calculated a weighted average of the pawprints' K_s magnitudes to obtain the 'tile' K_s, which then represented one epoch of data. During this process particular care was devoted to the determination of a proper Heliocentric Julian Day (HJD) for the K_s value of each 'tile' per epoch (see M12 for details).

The second phase of the 'Expérience pour la Recherche d'Objets Sombres' (EROS-2; Tisserand et al. 2007) is, at present, the largest optical[2] survey covering a large fraction of the LMC, and reaching out to peripheral areas such as the SEP region (see fig. 4 of M12). The 30 Dor field is covered, instead, by both the EROS-2 and

[1] http://horus.roe.ac.uk/versus/

[2] The EROS-2 *blue* channel (420–720 nm) overlaps with the *V* and *R* standard bands, and the *red* channel (620–920 nm) roughly matches the mean wavelength of the Cousins *I* band (Tisserand et al. 2007).

Table 1. Sample time series photometry for the Cepheid VMC J053048.71−694848.0 in the 30 Dor field.

HJD −240 0000	K_s	Err$_{K_s}$
55140.75594	14.347	0.007
55141.77415	14.477	0.007
55143.74588	14.310	0.006
55147.79060	14.394	0.006
55152.80550	14.288	0.007
55155.72048	14.285	0.007
55161.83663	14.336	0.007
55164.77643	14.473	0.007
55172.74263	14.291	0.006
55191.73701	14.280	0.006
55209.66414	14.425	0.007
55227.56999	14.263	0.006
55246.58263	14.275	0.006
55266.51279	14.277	0.006
55510.79965	14.398	0.007

The table is published in its entirety as Supporting Information with the electronic version of the article. A portion is shown here for guidance regarding its form and content.

the third phase of the 'Optical Gravitational Lensing Experiment' (OGLE-III; Soszyński et al. 2008, 2009) survey. For our analysis we used identification, pulsation period and optical-band light curves from the EROS-2 photometric archive for the classical Cepheids contained in the SEP; however, we opted to use the OGLE-III information, which is available in standard Johnson–Cousins V, I bands, for the 30 Dor Cepheids.

As a result of the matching procedure between the VMC and the optical surveys' catalogues, we found 11 classical Cepheids (of which eight are FO and three are F pulsators) in the SEP field, and 323 in the 30 Dor region (of which 161 pulsate in the F mode, 139 pulsate in the FO, whereas 8 and 15 objects are mixed mode F/FO and FO/SO,[3] respectively). The very small number of Cepheids in the SEP field may give rise to concerns about the completeness of the SEP sample. Indeed, we checked whether new Cepheids could be identified from the VMC data alone; however, 12 epochs do not seem to be sufficient and the variability flag of the VSA (Cross et al. 2009) does not yet appear reliable enough for this purpose. On the other hand, this small number seems to be consistent with the very peripheral location of the SEP region, which is very far from the LMC bar, where most of the classical Cepheids are located. There are 324 classical Cepheids in the OGLE-III catalogue of the 30 Dor tile, of which we recovered 323. Thus, in this field we are 99.7 per cent complete.

Time series K_s photometry for these variables is provided in Table 1, which is published in its entirety in the online version of the paper.

Our K_s photometry is in the VISTA system, which is tied to the Two Micron All Sky Survey, (2MASS; Skrutskie et al. 2006) photometry, with the difference in K_s magnitude only mildly depending on the $(J - K_s)$ colour. Indeed, the empirical results available to date[4] show that $(J - K_s)$ (2MASS) $= 1.081(J - K_s)$(VISTA) and K_s(2MASS) $= K_s$(VISTA)$-0.011(J - K_s)$(VISTA). In the absence of a complete light curve in J (only very few phase points are available in this passband), this correction might introduce errors larger than the correction itself. Indeed, for the typical $(J - K_s)$ colour of classical Cepheids with periods shorter than 20–30 d ($J - K_s \sim$ 0.3–0.4 mag), the correction is of the order of 3–4 mmag; hence, for Cepheids, to a very good approximation, the VISTA system reproduces well the 2MASS one at K_s. Furthermore, this error for the Cepheids is much smaller than the typical uncertainties of the *PL*, *PW* and *PLC* relations (see next sections).

The periods available from the EROS-2 and OGLE-III catalogues were used to fold the K_s-band light curves produced by the VMC observations of the SEP and 30 Dor variables, respectively. Examples of the VMC K_s-band light curves of the Cepheids in the 30 Dor and SEP regions are shown in Fig. 1 (see also Ripepi et al. 2012, for additional examples). The light curves are very well sampled and nicely shaped. Intensity-averaged $\langle K_s \rangle$ magnitudes were derived from the light curves simply using custom software written in C, which performs a spline interpolation to the data. Final $\langle K_s \rangle$ magnitudes are provided in Tables 2 and 3 for the 30 Dor and SEP classical Cepheids, respectively, along with the stars' main characteristics: VMC Id, coordinates, pulsation mode, $\langle V \rangle$ and $\langle I \rangle$ (for the 30 Dor Cepheids only) intensity-averaged magnitudes, period, K_s-band amplitude and individual $E(V - I)$ reddenings (for the 30 Dor Cepheids only; see the next section). The predominance of FO (eight) with respect to F (four) pulsators, as well as the lack of Cepheids with periods longer than 4 d in the SEP field are both remarkable. This might be related to the specific SFH in the SEP region (see M12 for details).

In the VMC data, a significant departure from linearity due to saturation starts around $K_s \sim 11.5$ mag, the actual value depending on seeing, airmass etc. (see Paper I). This limits the Cepheids that can be analysed on the basis of the VMC data to variables with pulsation period shorter than 20–30 d. The longest-period classical Cepheids analysed in the present paper has a variability period of 23 d. However, this threshold was mainly set by the lack of longer period pulsators in the OGLE-III and EROS-2 catalogues for the 30 Dor and SEP fields, rather than by the VMC saturation limit.

Fig. 2 shows the period range covered by the SEP (red filled triangles) and 30 Dor (black filled circles) classical Cepheids, over the full range of periods spanned by the LMC Cepheids (grey filled circles), according to the OGLE-III catalogue (Soszyński et al. 2008). The variables in the SEP and 30 Dor fields appear to sample very well the full distribution of LMC Cepheids with periods shorter than 20–30 d, thus ensuring a large significance of the *PL*, *PW* and *PLC* relations presented in the present study, which were extended beyond the period limit of 20–30 d set by the saturation threshold of the VMC K_s exposures by complementing the SEP and 30 Dor samples with classical Cepheids exceeding the 10-d period from Persson et al. (2004, see Section 3).

3 CLASSICAL CEPHEIDS IN THE 30 DOR FIELD

The *PLK* relations of the 172 F and 154 FO[5] classical Cepheids in the 30 Dor field are shown in Fig. 3. In order to extend the period coverage beyond the limit of 23 d set by the longest-period pulsator in our sample, we have complemented our data with the sample of Persson et al. (2004) which includes 84 F-mode Cepheids with

[3] SO means Second Overtone pulsator.

[4] http://casu.ast.cam.ac.uk/surveys-projects/vista/technical/photometric-properties

[5] Double-mode pulsators F/FO and FO/SO were included in the F and FO samples, respectively.

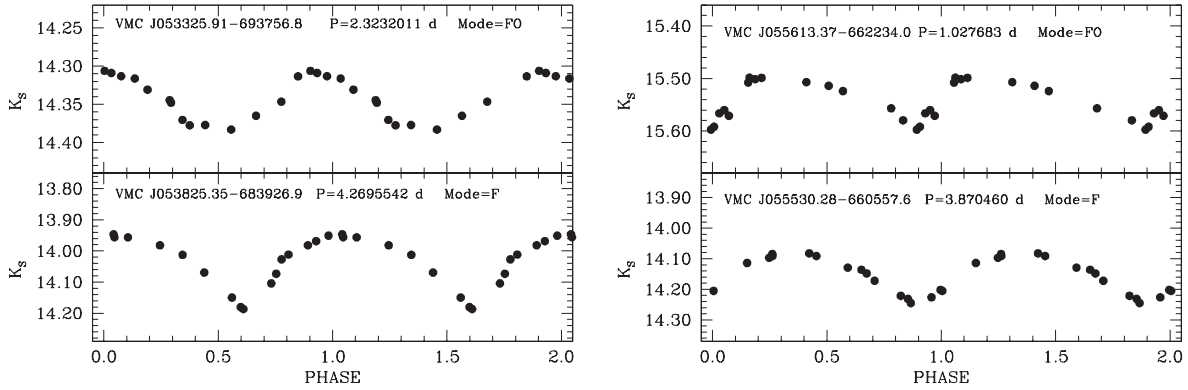

Figure 1. Examples of light curves for Cepheids in the 30 Dor (left panels) and SEP (right panels) fields, respectively. Errors of the single-epoch data are of the same size as the data points. Periods are from the OGLE-III survey for the 30 Dor Cepheids (Soszyński et al. 2008, 2009) and from the EROS-2 survey for the SEP variables (Marquette et al. 2009).

Table 2. Results for classical Cepheids in the 30 Dor field. M: pulsation mode. The complete table is available as Supporting Information with the electronic version of the article. An 'a' in the last column means that the star was not used to derive the *PL*, *PW* and *PLC* relations.

ID	RA (J2000)	Dec. (J2000)	M	$\langle I\rangle$ (mag)	$\langle V\rangle$ (mag)	Period (d)	$\langle K_s\rangle$ (mag)	$A(K_s)$ (mag)	$\sigma_{\langle K_s\rangle}$ (mag)	$E(V-I)$ (mag)	Notes
VMC J053048.71−694848.0	82.70296	−69.81333	F	15.354	16.105	3.240 862	14.353	0.22	0.006	0.08	
VMC J053059.48−693531.2	82.74783	−69.59200	F	14.890	15.693	4.656 827	13.917	0.22	0.008	0.09	
VMC J053100.91−694532.4	82.75379	−69.75900	F	14.724	15.453	4.874 545	13.775	0.23	0.004	0.08	
VMC J053101.03−690630.3	82.75429	−69.10842	F	15.779	16.722	3.130 618	14.589	0.12	0.007	0.12	
VMC J053101.70−690621.5	82.75708	−69.10597	F	15.993	17.003	2.908 321	14.694	0.20	0.010	0.12	
VMC J053102.99−693207.2	82.76246	−69.53533	F	14.816	15.547	4.641 402	13.957	0.25	0.009	0.09	
VMC J053112.67−700427.3	82.80279	−70.07425	F	14.949	15.679	4.226 975	14.041	0.22	0.008	0.02	
VMC J053117.49−695428.3	82.82287	−69.90786	F	14.357	15.133	5.976 499	13.388	0.21	0.004	0.10	
VMC J053118.30−693626.4	82.82625	−69.60733	F	14.875	15.716	4.834 38	13.833	0.14	0.008	0.10	
VMC J053122.41−695323.0	82.84337	−69.88972	F	15.058	15.643	3.408 864	14.120	0.19	0.009	0.10	

Table 3. Results for classical Cepheids in the SEP field.

ID	RA (J2000)	Dec. (J2000)	M	$\langle V\rangle$ (mag)	Period (d)	$\langle K_s\rangle$ (mag)	$A(K_s)$ (mag)	$\sigma_{\langle K_s\rangle}$ (mag)
VMC J055635.76−654742.2	89.14900	−65.79506	FO	16.596	1.188 733	15.264	0.09	0.0037
VMC J055711.13−655116.1	89.29636	−65.85448	FO	16.561	1.044 436	15.284	0.10	0.0040
VMC J055638.33−660302.5	89.15971	−66.05070	FO	16.640	1.214 786	15.338	0.08	0.0040
VMC J055530.28−660557.6	88.87615	−66.09933	F	15.785	3.870 460	14.145	0.15	0.0062
VMC J055613.37−662234.0	89.05570	−66.37611	FO	16.944	1.027 683	15.533	0.10	0.0060
VMC J060325.16−663124.5	90.85483	−66.52348	FO	16.677	1.277 076	15.224	0.14	0.0154
VMC J060318.77−665244.3	90.82822	−66.87896	FO	15.096	3.227 865	13.631	0.09	0.0045
VMC J060117.35−665319.9	90.32228	−66.88885	F	15.986	4.085 779	13.900	0.03	0.0070
VMC J055922.13−665709.6	89.84220	−66.95267	FO	16.100	1.683 674	14.788	0.11	0.0032
VMC J055535.43−670217.4	88.89761	−67.03818	F	17.009	3.902 331	14.130	0.02	0.0079
VMC J055942.93−670346.8	89.92889	−67.06300	FO	15.767	1.907 595	14.515	0.09	0.0023

periods mainly ranging between 10 and 100 d. To merge the two samples we first transformed Persson et al.'s original photometry from the Las Campanas Observatory (LCO) to the 2MASS system using the relations of Carpenter (2001). These data are shown as blue filled circles in Fig. 3. Inspection of this figure (or equivalently Fig. 4 or 5) and the straight line fits to the two sets of data shows no obvious discontinuity between the data, indicating that our approximation K_s(VISTA) ≈ K_s(2MASS) does not introduce a significant error.

To account for the variable reddening which characterizes the 30 Dor field, we adopted the recent evaluations by Haschke, Grebel & Duffau (2011) (reported in column 11 of Table 2), while to correct the Persson et al. (2004) data set we adopted the reddening values provided by the authors. We have verified that the two reddening systems are consistent with each other within a few hundredths of a mag, and that there is no trend with period.

Finally, we performed least-squares fits to the data of F- and FO-mode variables separately, adopting an equation of the form $K_s^0 = \alpha + \beta \log P$. The coefficients derived from the fits are provided in the first portion of Table 4.

In addition to the *PL* relation in the K_s band, we can consider the *PW* and *PLC* relations. The advantages of using these relations in place of a simple *PL* relation have been widely discussed in the literature (see e.g. Sandage & Tammann 1968; Madore 1982; Caputo, Marconi & Musella 2000; Marconi, Musella & Fiorentino 2005; Ngeow & Kanbur 2005; Bono et al. 2008, 2010; Sandage, Tammann & Reindl 2009; Ngeow 2012). These relations include a

© 2012 The Authors, MNRAS **424,** 1807–1816
Monthly Notices of the Royal Astronomical Society © 2012 RAS

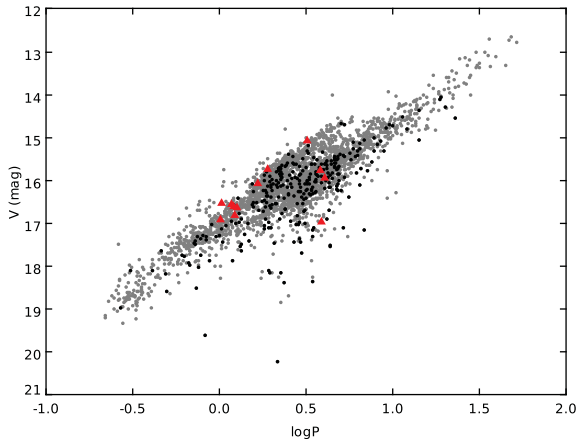

Figure 2. Period range covered by the SEP (red filled triangles) and 30 Dor (black filled circles) classical Cepheids, over the full range of periods spanned by the LMC classical Cepheids (grey filled circles), according to the OGLE-III catalogue (Soszyński et al. 2008, 2009). In this and the following figures, the periods are in day unit.

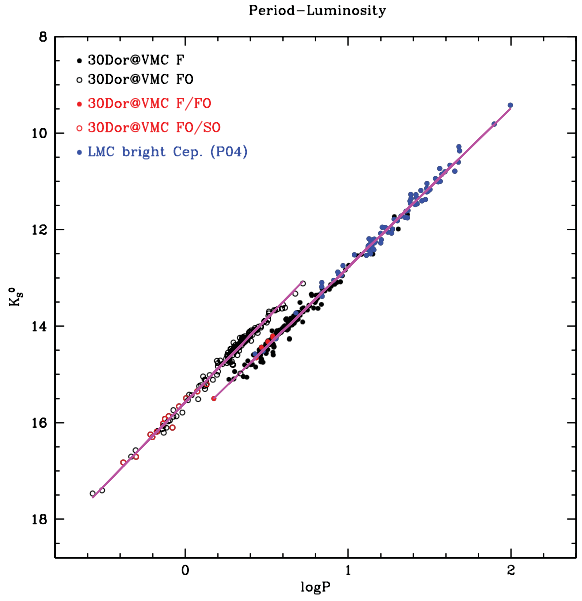

Figure 3. K_s-band *PL* relation for Cepheids in the 30 Dor field. Black open and filled circles show FO- and F-mode pulsators, respectively. Blue filled circles show the F-mode Cepheid sample of Persson et al. (2004). The solid lines are the result of the least-squares fit to the data (see text for details).

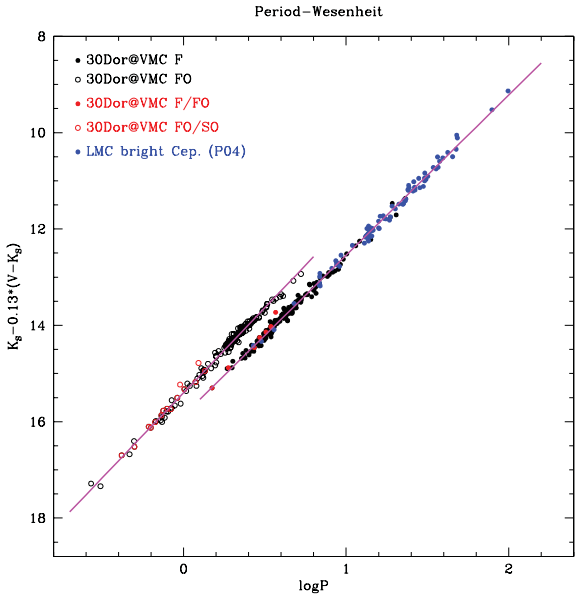

Figure 4. *PW* relation for Cepheids in the 30 Dor field. Symbols are as in Fig. 3.

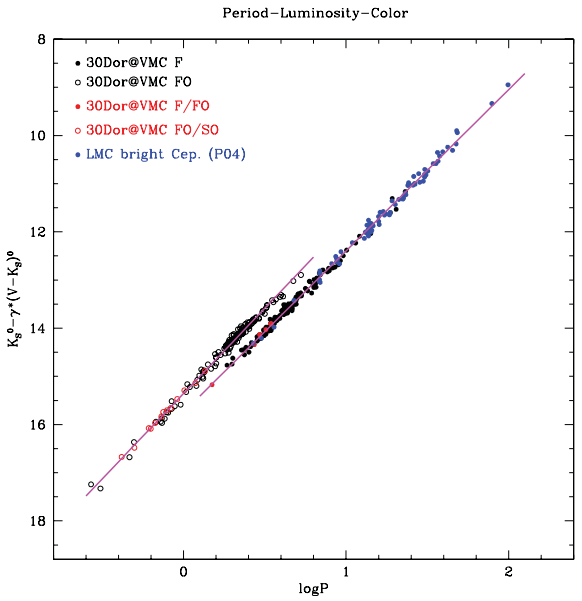

Figure 5. *PLC* relation for Cepheids in the 30 Dor field. Symbols are as in Fig. 3.

colour term with a coefficient that, in the case of the *PLC* relations, takes into account the colour distribution of the variable stars within the instability strip, whereas in the case of the Wesenheit functions it corresponds to the ratio between total to selective extinction in the filter pair (Madore 1982; Caputo et al. 2000), thus making the Wesenheit relations reddening free. We emphasize that these tools are particularly suited to studying the 3D structure of the Magellanic system, as they have much smaller dispersions than a simple *PL* relation (Caputo et al. 2000; Marconi et al. 2005; Bono et al. 2010).

The *PW* and *PLC* relations are usually calculated using the $(V - I)$ colour. However, given the data available to us, we have built our relations using the $V - K_s$ colour. As far as we know, this is the first empirical *PW* relation using such a colour. Following Cardelli, Clayton & Mathis (1989), the Wesenheit function is defined as $W(V, K_s) = K_s - 0.13(V - K_s)$, which is correlated with the logarithm of the period according to a linear relation of the form $W(V, K_s) = \alpha + \beta \log P$. Similarly, we adopt a *PLC* relation of the form $K_s^0 = \alpha + \beta \log P + \gamma(V - K_s)_0$. The coefficients of the relations derived with this procedure are provided in the middle and lower portions of Table 4. The relations are shown in Figs 4 and 5, respectively.

We point out that in deriving the above relations we decided to not apply any corrections for the inclination of the LMC disc to Persson et al. (2004)'s and our 30 Dor Cepheids, since our attempt to calculate e.g. the PW relation after de-projecting both Cepheid samples with the widely adopted van der Marel & Cioni (2001) or van der Marel et al. (2001) model parameters resulted in an increased rms dispersion of the relation. This is likely because

© 2012 The Authors, MNRAS **424,** 1807–1816
Monthly Notices of the Royal Astronomical Society © 2012 RAS

Table 4. *PL*, *PW* and *PLC* relations for F and FO classical Cepheids. The Wesenheit function is defined as $W(V, K_s) = K_s - 0.13(V - K_s)$.

Mode	α	σ_α	β	σ_β	γ	σ_γ	rms
			$K_s^0 = \alpha + \beta \log P$				
F	16.070	0.017	−3.295	0.018			0.102
FO	15.580	0.012	−3.471	0.035			0.099
			$W(V, K_s) = \alpha + \beta \log P$				
F	15.870	0.013	−3.325	0.014			0.078
FO	15.400	0.008	−3.530	0.025			0.070
			$K_s^0 = \alpha + \beta \log P + \gamma(V - K_s)_0$				
F	15.740	0.073	−3.346	0.013	0.216	0.014	0.073
FO	15.355	0.070	−3.545	0.026	0.163	0.014	0.070

current model uncertainties introduce errors of comparable size as the corrections themselves. In our particular case, as Persson et al. (2004)'s Cepheids are spatially well distributed over the whole LMC, their use should not introduce any systematics on the distance to the LMC barycentre. On the other hand, according to the aforementioned LMC disc models, the 30 Dor field is displaced off the LMC barycentre by, on average, only ∼0.02 mag [see also table 3 in Rubele et al. 2012, who performed similar calculations using the comparison between observed and simulated colour magnitude diagrams (CMDs)]. Such an effect is much smaller than the intrinsic scatter of the *PW* relations. We therefore believe that the relations in Table 4 can be safely applied to estimate the distance to the LMC barycentre.

We can now compare our results with previous studies. The literature values for the coefficients of the *PL*, *PW* and *PLC* relations are summarized in Table 5. The first four rows in the table report the empirical results for the PLK_s relation of F pulsators by Groenewegen (2000), Persson et al. (2004), Testa et al. (2007) and Storm et al. (2011b), while the fifth row shows the theoretical results by Caputo et al. (2000). Similarly, rows 6 and 7 display the empirical results by Groenewegen (2000) and the semi-empirical results by Bono et al. (2002), for FO pulsators. A comparison between Tables 4 and 5 reveals that for the PLK_s relation of the F-mode pulsators, there is general agreement within the errors between our results and Groenewegen (2000), Persson et al. (2004) and Storm et al. (2011b) (only slope for the latter because the zero-point is given in absolute magnitude). Only marginal agreement is found instead with Testa et al. (2007), whose results are based on the Persson et al. (2004) sample complemented at shorter periods by Cepheids belonging to the LMC clusters NGC 1866 and NGC 2031. This is likely due to the significantly larger sample, both at short and medium periods, presented in the present paper. As for the comparison with theory, we find that there is a satisfactory agreement between our slope and the slope predicted by pulsation models for the LMC's chemical composition (Caputo et al. 2000). The errors in the coefficients of our PLK_s relation are shorter than those in previous studies. This is a result of the large range in period spanned by the Cepheids in our sample, including for the first time a significant number of objects with NIR photometry and periods shorter than 5 d, and the very good sampling of our multi-epoch K_s light curves. In the case of the FO pulsators, the agreement with Groenewegen (2000) is less satisfactory than that for the F-mode Cepheids. This may be due to the advantage of the deeper magnitude limit achieved by the VMC survey, which allowed us to reach the fainter FO Cepheids populating the short-period tail of the PLK_s relation, along with the much better sampling of our K_s light curves. The Groenewegen (2000) relations rely in fact on 2MASS and Deep Near-Infrared Southern Sky Survey (DENIS; Epchtein et al. 1999) single-epoch NIR data; thus, the Cepheid's mean magnitude is, in principle, less well determined, increasing in turn the rms of the PLK_s relation. This is a natural consequence of studying Cepheids in the NIR using only single-epoch data.

Since there are no empirical *PW* and *PLC* relations in K_s available in the literature, we can only compare our relations with the theoretical results by Caputo et al. (2000). The slope of our $W(V, K_s)$ relation is in agreement with the theoretical value, while a significant discrepancy is found in the case of the *PLC* relation (see Table 5). This discrepancy could be due, at least in part, to uncertainties affecting the $(V - K_s)$-temperature transformations that might

Table 5. Literature values for the coefficients of the *PL*, *PW* and *PLC* relations, for F and FO Classical Cepheids. The Wesenheit function is defined as $W(V, K_s) = K_s - 0.13(V - K_s)$. Note that the photometry of previous studies was converted to the 2MASS system, for consistency with our results (see Section 2).

Mode	α	σ_α	β	σ_β	γ	σ_γ	rms	Source
				$K_s^0=\alpha+\beta\ \log P$				
F	16.032	0.025	−3.246	0.036			0.168	Groenewegen (2000)[a]
F	16.051	0.05	−3.281	0.040			0.108	Persson et al. (2004)[b]
F	15.945	0.040	−3.19	0.040				Testa et al. (2007)[b]
F	−2.36	0.04	−3.28	0.09			0.21	Storm et al. (2011b) [c]
F	−2.65	0.01	−3.23	0.01			0.07	Caputo et al. (2000)[d]
FO	15.533	0.032	−3.381	0.076			0.137	Groenewegen (2000) [a]
FO	15.62	0.13	−3.57	0.03			0.14	Bono et al. (2002)[a]
				$W(V, K_s) = \alpha + \beta \log P$				
F	−2.92	0.09	−3.21	0.04			0.09	Caputo et al. (2000)
				$K_s^0 = \alpha + \beta \log P + \gamma(V - K_s)_0$				
F	−3.37	0.04	−3.60	0.03	0.61	0.03	0.03	Caputo et al. (2000)

[a]Data in the CIT system: $K_s(2MASS) = K(CIT) - 0.024$ (Carpenter 2001).
[b]Data in the LCO system: $K_s(2MASS) = K_s(LCO) - 0.01$ (Carpenter 2001).
[c]Data in the SAAO system: $K_s(2MASS) = K(SAAO) + 0.02(J - K)(SAAO) - 0.025$ (Carpenter 2001).
[d]Models transformed to the Johnson system: for Cepheids $K(Johnson) \approx K(SAAO)$ (Bessell & Brett 1988).

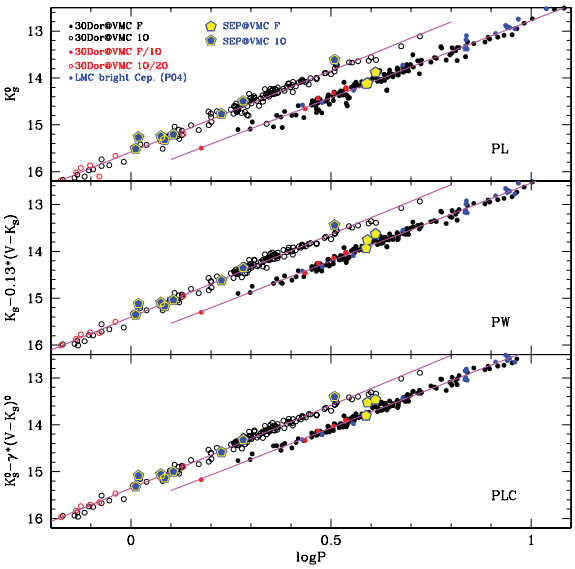

Figure 6. Classical Cepheids (blue and yellow pentagons for F and FO pulsators, respectively) in the SEP field overplotted on the *PL*, *PW* and *PLC* relationships defined by the 30 Dor Cepheids.

overestimate the coefficient of the predicted colour term and, in turn, the linear regression of the corrected magnitude versus period. This effect is expected to be mitigated in the Wesenheit approach thanks to the adoption of the same colour coefficient (in the empirical and theoretical relations) set by the Cardelli law.

Finally, we note that no statistically significant evidence is found for the *PL* discontinuity around 10 d claimed by several authors. Ngeow et al. (2005) performed a statistical study of the LMC Cepheid sample obtained from the MACHO data base (Alcock et al. 2000) and found that the observed behaviour in the period–magnitude diagrams is best reproduced by two linear relations, with a break at 10 d. A similar deviation from linearity is predicted by non-linear convective pulsation models (see e.g. Caputo et al. 2000; Fiorentino et al. 2002; Marconi et al. 2005, 2010), which also suggests a quadratic form of the *PL* relations, particularly in the optical bands. However, all these authors predict that the NIR *PL* and *PW* relations are well approximated by linear relations (see also Ngeow, Kanbur & Nanthakumar 2008), as we confirm with the present study.

4 CLASSICAL CEPHEIDS IN THE SEP FIELD

The number of SEP Cepheids is too small (11 objects, see Table 3) to define independent *PL*, *PW* and *PLC* relations. We did not attempt to re-calculate the relations but simply compared the SEP Cepheids with those obtained from the 30 Dor variables. This is done in Fig. 6, where for the SEP Cepheids we have adopted the reddening value $E(B-V) = 0.06$ mag from Rubele et al. (2012).[6]

The SEP variables overlap well with the 30 Dor Cepheids in all panels of the figure. However, there are a few exceptions: stars VMC J055711.13−655116.1, VMC J055638.33−660302.5, VMC J055613.37−662234.0 and VMC J055922.13−665709.6 deviate by more than 2σ from the *PL*, *PW* and *PLC* relations obtained in the 30 Dor field, and appear to be closer to us by a few kpc. Indeed, from the analysis of the CMD data, Rubele et al. (2012) find the SEP field to be located on average 0.05 mag closer to us than the 30 Dor region, which is fully consistent with the results we find here from the Cepheids.

[6] No evaluation of the SEP field reddening is available from the Haschke et al. (2011) study.

5 CALIBRATION OF THE *PL*, *PW* AND *PLC* ZERO-POINTS

Our main goal is to use the classical Cepheids observed by the VMC (along with the RR Lyrae stars; M12) to trace the 3D geometry of the Magellanic system. However, this analysis would be premature with the few VMC tiles observed so far. Still, we can use the *PL*, *PW* and *PLC* relations derived in the previous section to estimate an absolute distance to the LMC, but first need to calibrate their zero-points. In the following, we shall use mainly the *PW* and *PLC* relations, as they appear to be less dispersed than the *PL* relation, and derive zero-point estimates, adopting for the first time the V, $(V - K_s)$ combination, and two 'direct techniques': the trigonometric parallaxes of Galactic Cepheids and the Baade–Wesselink method directly applied to LMC Cepheids.

5.1 Zero-points from the parallax of Galactic Cepheids

Accurate parallaxes for Galactic Cepheids are available for fewer than 20 objects, from observations with the *Hipparcos* satellite (van Leeuwen et al. 2007) and the *HST* (Benedict et al. 2007). To use these data for our purpose, we had to: (i) derive the K-band *PL* relation and, for the first time, the V, $(V - K_s)$- *PW* and *PLC* relations for these Cepheids; (ii) apply them to our sample taking into account that possible differences may exist in the slopes and zero-points, due to metallicity effects.

From the van Leeuwen et al. (2007) and Benedict et al. (2007) samples, we only retained stars with the most accurate parallax ($\delta\pi/\pi \leq 0.2$). For 10 stars in common between the two sets, we computed weighted averages of the parallaxes. Photometric data (including K-band photometry, transformed to the 2MASS K_s system according to Carpenter 2001) and individual reddening values for these stars were taken from Fouqué et al. (2007), while for the Lutz–Kelker corrections we followed Benedict et al. (2007). We then computed the *PL*, *PW* and *PLC* relations, by excluding from the fit the most deviating stars: α UMi and S Mus. This left us with a total number of 13 Galactic Cepheids. Their list is provided in Table 6. Inclusion in the fit of the three suspected FO stars (see Table 6) did not change the results significantly; hence, we kept these stars to increase the statistics. We also kept all binary objects (see Table 6). Excluding them would considerably reduce the statistical significance of our results. This limitation, due to the paucity of trigonometric parallaxes for Cepheids, will be directly addressed when the astrometric satellite *Gaia* is launched and goes into operation in 2013. We first calculated the regressions leaving all parameters free to vary. The colour term in the *PLC* relation turned out to be insignificant; thus, the *PL* and *PLC* relationships are identical and equal to $K_S^0 = -2.44 \pm 0.12 - (3.20 \pm 0.14)\log P$. Similarly, for the Wesenheit function we have $W(V, K_s) = -2.61 \pm 0.12 - (3.28 \pm 0.13)\log P$. Although rather uncertain, the slopes of these relations are in good agreement with our results from the 30 Dor Cepheids, within the errors. We thus adopted our slopes from the 30 Dor Cepheids for the *PL* and *PW* relations to derive the following weighted-average zero-points of the parallax-based relations:

$$K_s^0(\mathrm{F}) = -2.40 \pm 0.05 - (3.295 \pm 0.018)\log P, \quad (1)$$

$$W(V, K_s)(\mathrm{F}) = -2.57 \pm 0.05 - (3.325 \pm 0.014)\log P, \quad (2)$$

Table 6. Galactic Cepheids with known parallax, used to calibrate the *PL*, *PW* and *PLC* relations. The column named 'LK' gives the Lutz–Kelker corrections applied in this work. An 'FO' in the notes means that the star is a suspect first overtone, according to the compilation by Fernie et al. (1995). 'O', 'B' and 'V' mean that the star is a binary with known orbital elements, spectroscopic and visual, respectively; a ':' means that confirmation is needed. After Szabados (2003).

ID	π (arcsec)	σ_π (arcsec)	$\log P$ (d)	$\langle V\rangle$ (mag)	$\langle K\rangle$ (mag)	$E(B-V)$ (mag)	LK (mag)	Note
SU Cas	2.57	0.33	0.440	5.9700	4.1062	0.2590	−0.1649	FO, O
β Dor	3.26	0.14	0.993	3.7570	1.9430	0.0520	−0.0184	
RT Aur	2.40	0.19	0.572	5.4480	3.8962	0.0590	−0.0627	B:
ζ Gem	2.74	0.12	1.006	3.9150	2.1145	0.0140	−0.0192	V
ℓ Car	2.03	0.16	1.551	3.6980	1.0788	0.1470	−0.0621	
BG Cru	2.23	0.30	0.678	5.4590	3.8704	0.1320	−0.1810	FO, B
X Sgr	3.17	0.14	0.846	4.5640	2.5033	0.2370	−0.0195	O
W Sgr	2.30	0.19	0.880	4.6700	2.8101	0.1080	−0.0682	O
Y Sgr	2.13	0.29	0.761	5.7450	3.5695	0.1910	−0.1854	B
FF Aql	2.64	0.16	0.650	5.3730	3.4706	0.1960	−0.0367	O
T Vul	2.06	0.22	0.647	5.7530	4.1814	0.0640	−0.1141	B
DT Cyg	2.19	0.33	0.550	5.7750	4.4109	0.0420	−0.2271	FO
δ Cep	3.71	0.12	0.730	3.9530	2.3037	0.0750	−0.0105	V

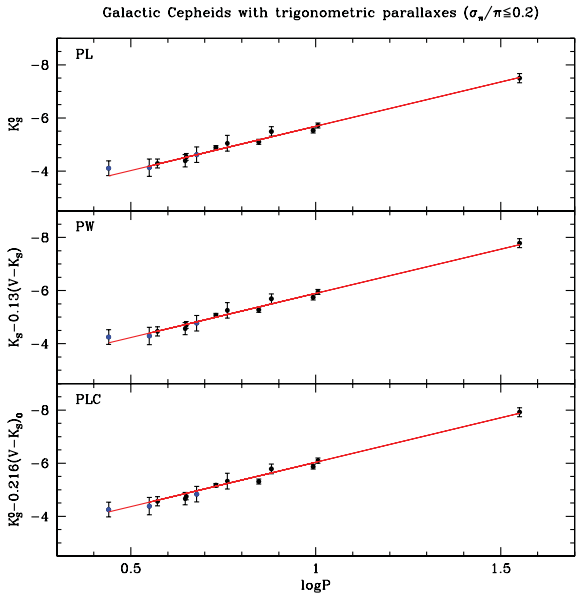

Figure 7. *PL*, *PW* and *PLC* relations for Galactic Cepheids with accurate trigonometric parallax. We have highlighted in blue the suspected FO-mode pulsators (see Table 6).

where the error on the zero-point is the standard deviation of the mean. Similarly, by adopting our values of 0.216 ± 0.014 and -3.346 ± 0.013 for the period and colour coefficients of the *PLC* relation, we obtained

$$K_s^0 = -2.69 \pm 0.05 - (3.346 \pm 0.013)\log P + (0.216 \pm 0.014)(V - K_s)_0. \quad (3)$$

Here, the errors on the zero-point estimates include the contribution of the systematic uncertainty due to the adoption of the same slope for Galactic and LMC Cepheids according to the model predictions by Caputo et al. (2000). The *PL*, *PW* and *PLC* relations obtained with this procedure are shown in Fig. 7. By comparing equations (2) and (3) with the results in Table 4, we obtain distance moduli of the LMC, based on the F-mode Cepheids, of $(m-M)_0^{\rm TRIG}(PW) = 18.44 \pm 0.05$ mag and $(m-M)_0^{\rm TRIG}(PLC) = 18.43 \pm 0.05$ mag, respectively.

5.2 Zero-points from the Baade–Wesselink method

5.2.1 *Infrared Surface Brightness (IRSB) formulation*

Recently, Storm et al. (2011a,b) published individual distances to Galactic and LMC Cepheids (36 objects in the LMC), based on application of the IRSB modification of the Baade–Wesselink technique (see e.g. Gieren, Fouqué & Gomez 2007 and references therein) to a sample of Galactic and LMC Cepheids and a new evaluation of the projection factor (*p*-factor) that transforms the observed radial velocity into pulsation velocity. We have used their absolute magnitudes in K[7] and V to calibrate the zero-points of the *PL*, *PW* and *PLC* relations. As done with the Galactic Cepheids, we adopted our slopes for the relations and determined their zero-points. The assumption is well justified in this case as both our and Storm et al. (2011b)'s Cepheids belong to the LMC; hence, we do not expect any metallicity effect. As a result, we obtain

$$K_s^0({\rm F}) = -2.40 \pm 0.07 - (3.295 \pm 0.018)\log P, \quad (4)$$

$$W(V, K_s)({\rm F}) = -2.60 \pm 0.07 - (3.325 \pm 0.014)\log P, \quad (5)$$

$$K_s^0(F) = -2.72 \pm 0.07 - (3.346 \pm 0.013)\log P + (0.216 \pm 0.014)(V - K_s)_0, \quad (6)$$

where the errors on the zero-points include the dispersion of the measurements, as well as an estimate of the systematic error due to the uncertainty on the *p*-factor (see e.g. Storm et al. 2011a and references therein). The new zero-points are in excellent agreement with those derived from the Galactic Cepheids and confirm Storm et al. (2011a)'s findings. These relations lead to distance moduli for the LMC of $(m-M)_0^{\rm IRSB}(PW) = 18.46 \pm 0.07$ mag and $(m-M)_0^{\rm IRSB}(PLC) = 18.46 \pm 0.07$ mag, respectively, in very good agreement with Storm et al. (2011b).

[7] Note that these K magnitudes were transformed to the 2MASS K_s system and referred to the centre of the LMC using the corrections by Storm et al. (2011b).

5.2.2 CORS Baade–Wesselink formulation

A different implementation of the Baade–Wesselink technique, the so-called CORS method (see e.g. Caccin et al. 1981; Ripepi et al. 1997; Molinaro et al. 2011), was applied by Molinaro et al. (2012) to nine Cepheids (seven F mode and two FO mode) belonging to NGC 1866, a populous widely studied young cluster located about 4.1° north-west of the LMC bar. These authors find $(m - M)_0(\mathrm{NGC\,1866}) = 18.51 \pm 0.03$ mag. This value can be used to calibrate the *PL*, *PW* and *PLC* relations following the same procedure as described in the previous sections, and with the advantage that we can now also calibrate the relation for FO pulsators (although only based on two stars). In this case we obtain

$$K_s^0(\mathrm{F}) = -2.44 \pm 0.07 - (3.295 \pm 0.018) \log P, \quad (7)$$

$$K_s^0(\mathrm{FO}) = -2.94 \pm 0.07 - (3.471 \pm 0.035) \log P, \quad (8)$$

$$W(V, K_s)(\mathrm{F}) = -2.62 \pm 0.07 - (3.325 \pm 0.014) \log P, \quad (9)$$

$$W(V, K_s)(\mathrm{FO}) = -3.10 \pm 0.07 - (3.530 \pm 0.025) \log P, \quad (10)$$

$$K_s^0(\mathrm{F}) = -2.74 \pm 0.07 - (3.346 \pm 0.013) \log P + (0.216 \pm 0.014)(V - K_s)_0, \quad (11)$$

$$K_s^0(\mathrm{FO}) = -3.15 \pm 0.07 - (3.545 \pm 0.026) \log P + (0.163 \pm 0.014)(V - K_s)_0. \quad (12)$$

Here, as in the previous section, the errors in the zero-points include both the dispersion of the measures and the uncertainty in the *p*-factor.

Averaging the results for F and FO Cepheids, we obtain distance moduli of $(m - M)_0^{\mathrm{CORS}}(PW) = 18.49 \pm 0.07$ mag and $(m - M)_0^{\mathrm{CORS}}(PLC) = 18.49 \pm 0.07$ mag, respectively. The marginally significant -0.02 mag difference with Molinaro et al. (2012) is likely due to the relative distance between NGC 1866 and the LMC centre. Indeed, a direct comparison of the NGC 1866 Cepheids with our *PL* relation reveals a difference of the order of -0.02 ± 0.02 mag. Such an uncertainty, when added in quadrature, has negligible effects compared to other sources of error.

6 DISCUSSION AND ESTIMATE OF THE DISTANCE TO THE LMC

In the previous sections, we have calibrated the zero-points of our *PL*, *PW* and *PLC* relations using different methods, and derived in turn different estimates of the distance to the LMC. By combining these results, we can derive our best estimates for the zero-points of the *PL*, *PW* and *PLC* relations, as well as for the distance to the LMC. In particular, a weighted mean of the zero-points for F-mode pulsators leads to the following final *PL*, *PW* and *PLC* relations:

$$K_s^0(\mathrm{F}) = -2.41 \pm 0.03 - (3.295 \pm 0.018) \log P, \quad (13)$$

$$W(V, K_s)(\mathrm{F}) = -2.59 \pm 0.03 - (3.325 \pm 0.014) \log P, \quad (14)$$

$$K_s^0(\mathrm{F}) = -2.71 \pm 0.03 - (3.346 \pm 0.013) \log P + (0.216 \pm 0.014)(V - K_s)_0. \quad (15)$$

As for the distance to the LMC, a similar weighted mean leads to the final value of $(m - M)_0 = 18.46 \pm 0.03$ mag, in excellent agreement with several independent literature results (see e.g. Walker 2012 and references therein). In particular, Walker (2012) in his recent review of current LMC distance estimates based on Cepheids, red variables, RR Lyrae, red clump stars and eclipsing binaries showed that most of these indicators agree on a mean value of the distance modulus for the LMC of 18.48 ± 0.05 mag.

7 SUMMARY AND CONCLUSIONS

We have presented first results for classical Cepheids observed by the VMC survey in two fields of the LMC, centred on the SEP and the 30 Dor regions, respectively. The identification of the variables and their optical magnitudes were derived from the EROS-2 and OGLE-III catalogues. Our Cepheid K_s light curves are very well sampled, with at least 12 epochs, and very precise, with typical errors of 0.01 mag, or better, for individual phase points. Our observing strategy allowed us to measure for the first time the K_s magnitude of the faintest Cepheids in the LMC, which are mostly FO pulsators, thus enabling us to obtain *PL*, *PW* and *PLC* relations defined over the whole period range spanned by the LMC FO Cepheids. Since the longest-period Cepheid in our data set is a 23-d variable, we have complemented our sample with data from Persson et al. (2004) for bright F-mode Cepheids. On this basis, we have built a *PL* relation in the K_s band that for the first time also includes short-period (i.e. low-luminosity) F pulsators. We have also calculated the first empirical *PL*, *PW* and *PLC* relations using the $(V - K_s)$ colour. The latter two have very small dispersion ($\leq$0.07 mag) and will be particularly suited for the 3D study of the Magellanic system, a main goal of the VMC project, which we cannot yet achieve with only two VMC fields completed so far. We have used 'direct' distance measures to both Galactic and LMC Cepheids to calibrate the zero-points of the *PL*, *PW* and *PLC* relations derived in this paper. This procedure led to equations (13)–(15) that we have used to estimate an absolute distance to the LMC of $(m - M)_0 = 18.46 \pm 0.03$ mag, in excellent agreement with the latest determinations of the LMC distance, based on classical Cepheids and other independent distance indicators.

The new final distance modulus for the LMC derived in the present study is slightly shorter than the value assumed by the *HST* Key Project (18.50 mag, according to Freedman et al. 2001), thus implying LMC-calibrated extragalactic distances shorter by about 2 per cent, a small but still non-negligible correction, in the era of the claimed Hubble constant within a few per cent uncertainty (see e.g. Riess et al. 2011).

ACKNOWLEDGMENTS

It is a pleasure to thank our referee B. Madore for his prompt and helpful report. VR warmly thanks Roberto Molinaro for providing the program for the spline interpolation of the light curves. MI Moretti thanks the Royal Astronomical Society for financial support during her two-month stay at the University of Hertfordshire. Financial support for this work was provided by PRIN-INAF 2008 (P.I. Marcella Marconi) and by COFIS ASI- INAF I/016/07/0. RdG acknowledges partial research support from the National Natural Science Foundation of China (grant 11073001). We thank the UK's VISTA Data Flow System comprising the VISTA pipeline at the Cambridge Astronomy Survey Unit (CASU) and the VISTA Science Archive at Wide Field Astronomy Unit (Edinburgh) (WFAU) provided calibrated data products, and is supported by STFC.

REFERENCES

Alcock C. et al., 2000, ApJ, 542, 281
Bekki K., Chiba M., 2007, MNRAS, 381, L16
Benedict G. F. et al., 2007, AJ, 133, 1810
Bessell M. S., Brett J. M., 1988, PASP, 100, 1134
Bono G., Caputo F., Castellani V., Marconi M., 1999, ApJ, 512, 711
Bono G., Groenewegen M. A. T., Marconi M., Caputo F., 2002, ApJ, 574, L33
Bono G., Caputo F., Marconi M., Musella I., 2008, ApJ, 684, 102
Bono G., Caputo F., Marconi M., Musella I., 2010, ApJ, 715, 277
Brocato E., Caputo F., Castellani V., Marconi M., Musella I., 2004, AJ, 128, 1597
Caccin R., Onnembo A., Russo G., Sollazzo C., 1981, A&A, 97, 104
Caputo F., Marconi M., Musella I., 2000, A&A, 354, 610
Cardelli J. A., Clayton G. C., Mathis J. S., 1989, ApJ, 345, 245
Carpenter J. M., 2001, AJ, 121, 2851
Cioni M.-R. L. et al., 2011, A&A, 527, 116 (Paper I)
Cross N. J. G., Collins R. S., Hambly N. C., Blake R. P., Read M. A., Sutorius E. T. W., Mann R. G., Williams P. M., 2009, MNRAS, 339, 1730
Cross N. J. G. et al., 2012, MNRAS, submitted
Dalton G. B. et al., 2006, SPIE Conf. Ser 6269, 30
Di Criscienzo M., Caputo F., Marconi M., Musella I., 2006, MNRAS, 365, 1357
Emerson J. P. et al., 2004, Proc. SPIE, 5493, 401
Emerson J. P., McPherson A., Sutherland W., 2006, Messenger, 126, 41
Epchtein N. et al., 1999, A&A, 349, 236
Fernie J. D., Beattie B., Evans N. R., Seager S., 1995, Inf. Bull. Var. Stars, 4148, 1
Fiorentino G., Caputo F., Marconi M., Musella I., 2002, ApJ, 576, 402
Fouqué P. et al., 2007, A&A, 476, 73
Freedman W. L., Madore B. F., 2011, ApJ, 734, 46
Freedman W. L. et al., 2001, ApJ, 553, 47
Gieren W. P., Fouqué P., Gomez M. I., 1997, ApJ, 488, 74
Groenewegen M. A. T., 2000, A&A, 363, 901
Harris J., Zaritsky D., 2004, AJ, 127, 1531
Harris J., Zaritsky D., 2009, AJ, 138, 1243
Haschke R., Grebel E. K., Duffau S., 2011, AJ, 141, 158
Irwin M. J. et al., 2004, Proc. SPIE, 5493, 411
Lindegren L., 2010, IAU Symp., 261, 296
Lindegren L., Perryman M. A. C., 1996, A&AS, 116, 579
Madore B. F., 1982, ApJ, 253, 575
Madore B. F., Freedman W., 1991, PASP, 103, 933
Marconi M., 2009, Mem. Soc. Astron. Ital., 80, 141
Marconi M., Musella I., Fiorentino G., 2005, ApJ, 632, 590
Marconi M. et al., 2010, ApJ, 713, 615
Marquette J.-B. et al., 2009, A&A, 495, 249
Molinaro R., Ripepi V., Marconi M., Bono G., Lub J., Pedicelli S., Pel J. W., 2011, MNRAS, 413, 942
Molinaro R. et al., 2012, ApJ, 748, 69
Moretti M. I. et al., 2012, MNRAS, submitted (M12)
Muller E., Stanimirović S., Rosolowsky E., Staveley-Smith L., 2004, ApJ, 616, 845
Neilson H. R., Langer N., 2012, A&A, 537, 26
Ngeow C.-C., 2012, ApJ, 747, 50
Ngeow C.-C., Kanbur S. M., 2005, MNRAS, 360, 1033
Ngeow C.-C., Kanbur S. M., Nikolae S., Buonaccorsi J., Cook K. H., Welch D. L., 2005, MNRAS, 363, 831
Ngeow C.-C., Kanbur S. M., Nanthakumar A., 2008, A&A, 477, 621
Persson S. E. et al., 2004, AJ, 128, 2239
Putman M. E. et al., 1998, Nat, 394, 752
Riess A. et al., 2011, ApJ, 730, 119
Ripepi V., Barone F., Milano F., Russo G., 1997, A&A, 318, 797
Ripepi V., Moretti M. I., Clementini G., Marconi M., Cioni M.-R. L., Marquette J. B., Tisserand P., 2012, Ap&SS, in press
Romaniello M., Primas F., Mottini M., Groenewegen M. A. T., Bono G., François P., 2005, A&A, 429, 37
Romaniello M., Primas F., Mottini M., Groenewegen M. A. T., Bono G., François P., 2008, A&A, 488, 731
Rubele S. et al., 2012, A&A, 537, 106 (Paper IV)
Saha A., Sandage A., Tammann G. A., Dolphin A. E., Christensen J., Panagia N., Macchetto F. D., 2001, ApJ, 562, 314
Sandage A., Tammann G., 1968, ApJ, 151, 531
Sandage A., Tammann G. A., Reindl B., 2009, A&A, 493, 471S
Skrutskie M. F. et al., 2006, AJ, 131, 1163
Soszyński I. et al., 2008, Acta Astron., 58, 163
Soszyński I. et al., 2009, Acta Astron., 59, 1
Stanimirović S., Staveley-Smith L., Jones P. A., 2004, ApJ, 604, 176
Storm J. et al., 2011a, A&A, 534, A94
Storm J., Gieren W., Fouqué P., Barnes T. G., Soszyński I., Pietrzyński G., Nardetto N., Queloz D., 2011b, A&A, 534, A95
Szabados L., 2003, Inf. Bull. Var. Stars, 5394, 1
Szewczyk O. et al., 2008, AJ, 136, 272
Testa V. et al., 2007, A&A, 462, 599
Tisserand P. et al., 2007, A&A, 469, 387
van der Marel R. P., Cioni M.-R. L., 2001, AJ, 122, 1807
van der Marel R. P., Alves D. R., Hardy E., Suntzeff N. B., 2002, AJ, 124, 2639
van Leeuwen F., Feast M. W., Whitelock P. A., Laney C. D., 2007, MNRAS, 379, 723
Walker A., 2012, Ap&SS, in press

SUPPORTING INFORMATION

Additional Supporting Information may be found in the online version of this article:

Table 1. Time series photometry.
Table 2. Results for classical Cepheids in the 30 Dor field.

Please note: Wiley-Blackwell are not responsible for the content or functionality of any supporting materials supplied by the authors. Any queries (other than missing material) should be directed to the corresponding author for the article.

This paper has been typeset from a TEX/LATEX file prepared by the author.